Development of Seismic Isolation System for Unloaders

R. Haymoz
Buhler AG, Uzwil, Switzerland

Y. Nishiyama, N. Niiyama & K. Ogata
Yacmo Co. Ltd., Tokyo, Japan

T. Fujita
Professor Emeritus, The University of Tokyo, Tokyo, Japan

SUMMARY:
This paper outlines development of a seismic isolation system for unloaders that are used to land grain from ships at piers. In Japan many unloaders received severe damage, such as collapse, in past destructive earthquakes. Therefore, the necessity for seismic protection is well recognized, and seismic isolation systems are used to protect unloaders against earthquake. In this project, a new type of seismic isolation system was developed for unloaders. Static tests of a full-scale model and dynamic tests of a scale model together were carried out, as were numerical analyses, and the system exhibited good isolation performance and reliability.

Keywords: Unloader, Seismic Isolation, Experiment, Scale model experiment, Modal analysis

1. INTRODUCTION

In this paper, we describe the development of a seismic isolation system for unloaders that are used to land grain from ships at piers. In Japan, many loading and unloading machines used at harbors, such as unloaders and container cranes, have received damage from past earthquakes. For example, container cranes at Kobe Port were seriously damaged by the Hanshin-Awaji Earthquake in 1995 (Fujimoto, 1995). As a result, the necessity of seismic measures for unloaders and container crane has promoted a variety of research efforts (Masuda et al., 2010). In view that such cargo handling machines at harbors are expected to play a role as a lifeline in the event of a disaster, seismic measures for them are essential.

The seismic isolation system we propose is a seismic isolator that is special to unloaders and isolates horizontal two-dimensional vibration. It incorporates a special locking mechanism into an oil damper to prevent the isolator from moving during normal operation of the unloader or by a strong wind. To verify the function and soundness of the system, in the development stage, we fabricated a full-scale model and conducted a static force-application test to check that it had sufficient stiffness and strength. Moreover, to verify the effect of the system, we used FEM analysis to clarify the modal characteristics of the unloader under consideration and fabricated a 1/8-scale model having similar modal characteristics to conduct a vibration experiment. The experiment results show that the isolator can effectively reduce the response acceleration of the unloader and suppress the uplift of the legs. We also used a two-mass model, conducted a simulation, and confirmed that the analysis results agree with the experimental results very well. According, we have found that our analysis method is effective and made it possible to work on the specifications of any isolator in advance.

2. DEVELOPMENT OF THE SEISMIC ISOLATOR FOR UNLOADERS

To conduct the static force-application test of the full-scale model of the isolator and the excitation experiment of the scale model, we selected an unloader shown in Fig. 2.1. Total mass was 400 tons, height was about 27 meters, and the distance between legs was 10 meters in both directions (parallel and perpendicular to the rail).

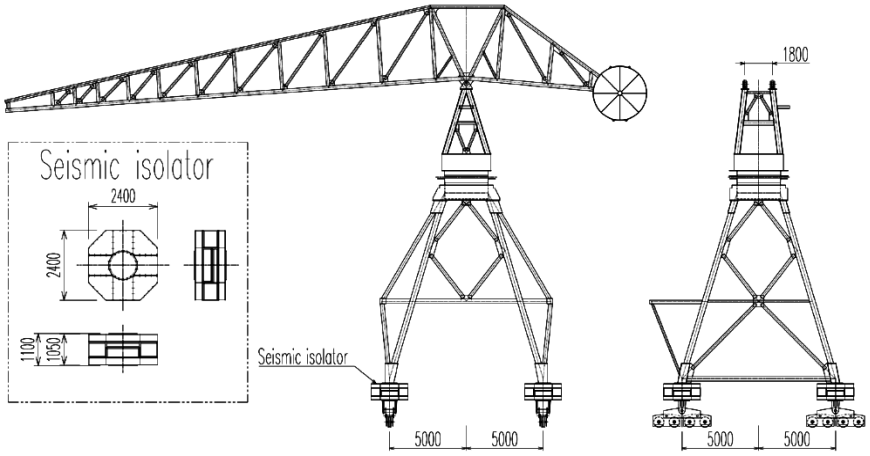

Figure 2.1. An unloader with seismic isolation systems employed in the study

2.1. Structure of the seismic isolator

Fig. 2.2 shows the structure and specifications of the isolator we developed. Two pairs of linear guiderails (four in total), which cross each other at right angles and which are attached to upper and lower frames, support a vertical load and realize a planar movement without rotation. Two pieces of laminated rubber, installed in respective directions, exert restoration force, while two pairs of oil dampers (four in total) attached to the upper and lower frames produce damping force. To avoid unnecessary movement during normal operation of the unloader or when strong wind rises, the oil damper has a locking mechanism that fixes the isolator until it receives a certain load. The full stroke of the isolator is ±300 mm. If the frame moves beyond full stroke, an oil buffer absorbs the shock.

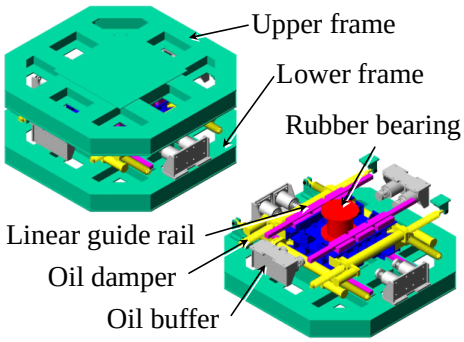

Specifications

Item	Specification
Size (W × D × H)	2400 × 2400 × 1000 mm
Admissible displacement	±300 mm
Weight	7000 kg

Figure 2.2. General view and specifications of the seismic isolation system for unloaders

2.2. Structural analysis with FEM

We used the Finite Element Method (FEM) to analyze the structure of the isolator we designed and to verify that it would be neither broken nor deformed at a load of twice the unloader's weight (1,960 kN per leg). Modeling the whole unit was complicated, so we created only a single frame model for FEM analysis, because the upper and lower frames have almost the same shape and boundary conditions, including force-application points. We employed midas/NFX, which uses NEi Nastran as an analysis engine and was provided by Midas. Fig. 2.3 shows the FEM analysis results when a maximum horizontal displacement and a vertical load of 1,960 kN were given to the isolator. Stress at a point marked by an orange flag was 342 MPa which exceeded the yielding point, although the plastic deformation of the frame was inconsiderable. Furthermore, it was expected that such stress concentration would not occur when taking into consideration the assumptions we made, including the approximation of linear block-supported part of the linear guide to a single point. We employed this design because the actual stress should be much lower.

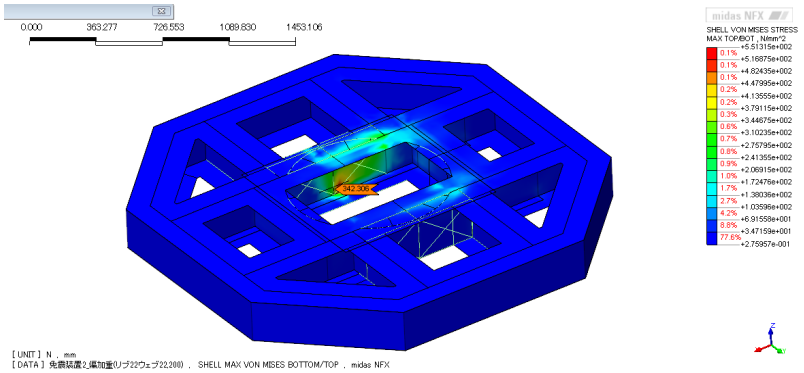

Figure 2.3. Von Mises stresses of the frame by FEM analysis under the conditions of a 1960 kN vertical load and a 0.3 m horizontal displacement

3. CONDUCTING A STATIC FORCE-APPLICATION TEST TO CHECK THE SYSTEM FOR FUNCTION AND SOUNDNESS

In the static force-application test of the full-scale model, we applied a strain gauge to the part having a large stress shown by the structural analysis with the FEM in order to measure the stress, to find the horizontal restoration force hysteresis of the isolator, and to verify the function of the locking mechanism of the oil damper.

3.1. Method and apparatus for the static force-application test of the full-scale model

Fig. 3.1 shows a static force-application tester for the full-scale model. The vertical actuator exerted a force of up to 1,960 kN on the isolator, while the horizontal actuator moved the lower frame of the isolator slowly. We restricted the vertical and horizontal slide tables so that the former imposed only vertical force on the isolator and the latter moved the lower frame along only the horizontal direction. A load cell attached to each actuator measured the actual force generated. The columns of the model reproduce the legs of the actual unloader, which produce an offset load because they are not vertical. We applied a strain gauge to the part (marked by the orange flag in Fig. 2.3) of the frame that had a large stress as expected by the FEM analysis, in order to measure it. The two measurement points on the upper frame are called SG1 and SG2, while those on the lower frame are called SG3 and SG4.

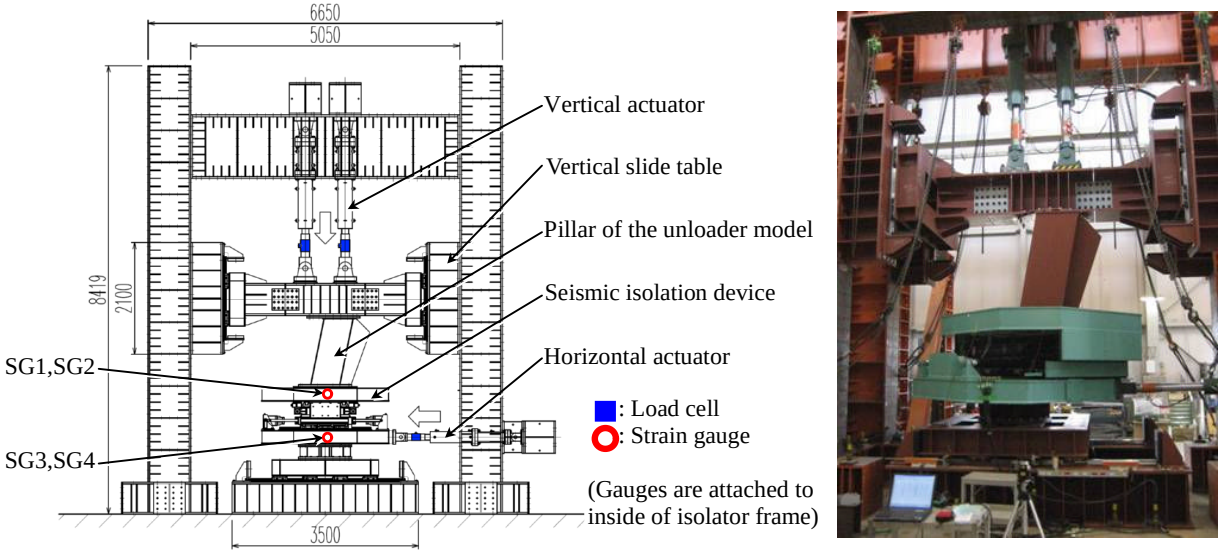

Figure 3.1. Test apparatus for static loading tests of full-scale seismic isolation device

3.2. Results of the force-application test and consideration

Fig. 3.2 (a) shows the resultant horizontal load-displacement curve when we installed the isolator in the tester so that the linear guide formed an angle of 45 degrees with respect to the loading direction of the horizontal actuator, exerted a vertical force of 1,960 kN, and let the lower frame make two round-trip displacements from the +400 mm position to the −100 mm position. Note that the reason why the positive displacement was larger than the negative displacement was that the stroke of the horizontal actuator was limited. The figure has an enlarged view of the origin and its vicinity, which shows that the horizontal displacement is small until the horizontal load is 90 kN. This is because of the locking mechanism of the oil damper, and confirmed that it worked properly. We conducted the test under two conditions: in one we moved the isolator horizontally at an angle of 45 degrees while applying an unloader load of 980 kN vertically, and in the other we moved only the lower linear guide along the sliding direction under a vertical load of 980 kN. The results gave us the spring constant of the isolator, which was 202 kN/m at a temperature of 20 degrees Celsius. In consideration of the mass of the unloader, the natural frequency of the seismic isolation system was 0.23 Hz. In addition, a performance test of the laminated rubber showed a spring constant of 218 kN/m at a temperature of 20 degrees Celsius, resulting in a natural frequency of 0.24 Hz. We confirmed that the two results were consistent with each other. Fig. 3.2 (b) shows the von Mises stress at SG2, which presented the largest frame strain among the measurement results. The peak is 150 MPa, which is smaller than the yielding point of 235 MPa shown by a dashed line. Therefore, we confirmed that the frame had sufficient stiffness.

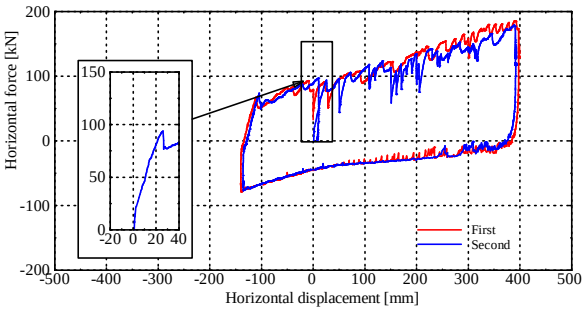

(a) Horizontal restoration force vs. horizontal displacement

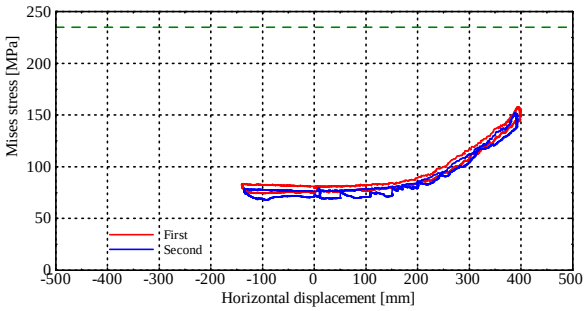

(b) Von Mises stress at SG2 point of the frame

Figure 3.2. Horizontal restoration force characteristics and von Mises stress of the frame under a 1960 kN vertical load and horizontal displacement in a direction at a 45° angle to the linear guide rails

4. SIMULATION WITH FEM ANALYSIS AND EXCITATION TEST OF THE SCALE MODEL

We conducted an excitation test on the 1/8 scale model of the unloader including the isolators not only to check whether they have isolating performance sufficiently high for practical use but also to build and validate an analytical model able to reproduce the seismic response of the isolated unloader.

4.1. Excitation test of the 1/8 scale model

4.1.1. Designing the scale model

Table 4.1 shows the resultant modal characteristics of the full-scale model of the unloader given by FEM analysis with midas/NFX. We designed the 1/8 scale model to reproduce such modal characteristics.

Table 4.1. FEM analysis result for a real unloader.

Modal parameter	X-direction (boom direction)	Y-direction (running rail direction)
Natural frequency [Hz]	1.6	0.75
Modal effective mass [kg]	476×10^3	372×10^3

We specified the scale of the model at one-eighth in consideration of the size of the shaking table. Table 4.2 lists the similitudes of acceleration, length, time, mass, and natural frequency (Iai, 1989).

Table 4.2. Similitudes for scale model excitation tests

Physical quantity	Unit	Dimension	Full-scale	1/n scale model	1/8 scale model
Acceleration	m/s^2	LT^{-2}	1	1	1
Length	m	L	1	1/n	1/8
Time	s	T	1	$1/\sqrt{n}$	$1/\sqrt{8}$
Mass	kg	M	1	$1/n^3$	$1/8^3$
Natural frequency	Hz	T^{-1}	1	$\sqrt{n}$	$\sqrt{8}$

To fabricate the 1/8 scale model from ready-made products, we prepared round bars and plates for all the components and adjusted the bar diameter and plate thickness so that the resultant model met the modal characteristics (natural frequency, effective mass, and mode shape) given by FEM analysis. Compared with the modal characteristics of the real unloader, the scale model should have natural frequencies of 4.5 Hz and 2.1 Hz in the boom (X) and running rail (Y) directions, respectively. In addition, we designed the scale model with FEM analysis so that it would have mode shapes as similar as possible to those of the real machine. The resultant model had the modal characteristics shown in Fig. 4.1. The natural frequency was a little higher in the Y direction and the effective mass was relatively small, but we thought that they were within an allowable range.

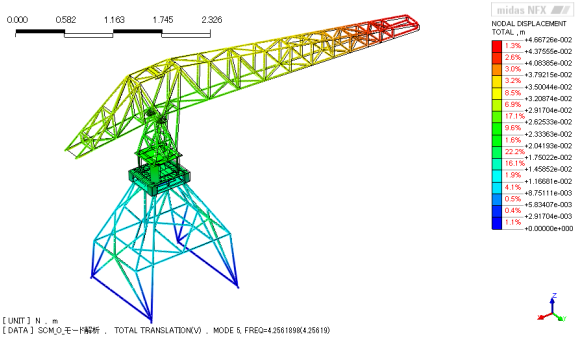

(a) Dominant mode in boom direction (X-dir.)
Natural frequency: 4.3 Hz
Modal effective mass：524 kg

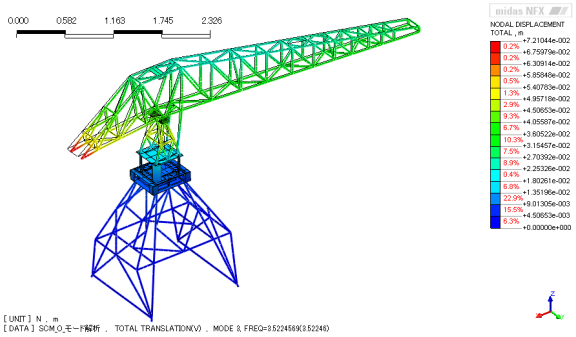

(b) Dominant mode in running rail direction (Y-dir.)
Natural frequency: 3.5 Hz
Modal effective mass: 372 kg

Figure 4.1. Dominant modes of 1/8 scale model

4.1.2. Excitation test method and tester

The left portion of Fig. 4.2 is a photograph of the 1/8 scale model actually mounted on the shaking table. The table under the photo shows the specifications of the model, and the right portion of the figure indicates measurement points, their labels, and the coordinate system. In the experiment, we put accelerometers to AX1 to AX3 and AY1 to AY3, load cells to LV1 to LV4, and a displacement sensor to DX1 and DX2. We measured the acceleration, the axial force acting on the legs, and the displacement of the isolator under two conditions: one was that the isolator was locked and the other was that it worked. We defined the coordinate system as shown in the figure and called the boom and running rail directions X and Y, respectively.

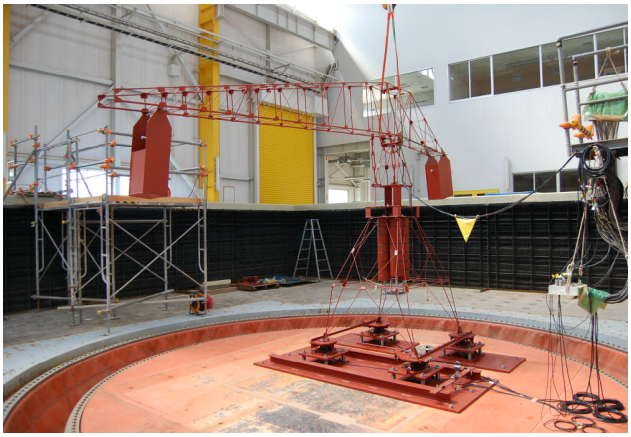

Specifications

Height	3100 mm
Width	1450 mm
Boom length	5200 mm
Weight	640 kg

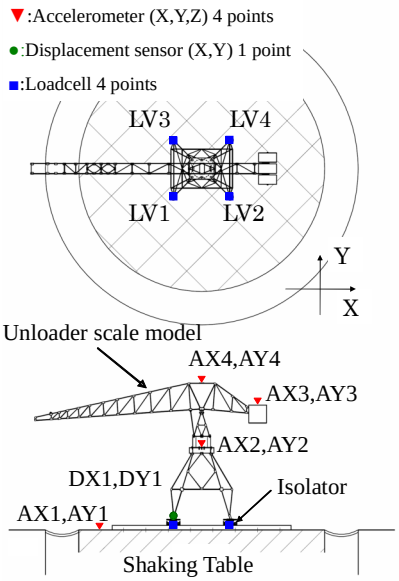

Figure 4.2. Excitation tests of 1/8 scale model

We selected some excitation inputs from past earthquake ground motion records and reduced the time scale to $1/\sqrt{8}$ according to the law of similarity. The scale model had a breaking risk if it was exposed to large acceleration in an excitation test without seismic isolation. To avoid this, we considered readings from the load cell to define the acceleration at which the leg floated as an upper limit, and determined the amplitude of each input to be used. Table 4.3 lists the inputs used for the excitation test. Note that we set them so that the maximum acceleration was given in the X direction.

Table 4.3. Inputs of shaking table used for excitation tests of 1/8 scale model

No	Name	Amplitude	Earthquake
1	Hachinohe	75%	1968 Tokachi-Oki, Japan
2	El-Centro	110%	1940 Imperial Valley, USA
3	Port Island	50%	1995 Kobe, Japan
4	JMA Kobe	18%	1995 Kobe, Japan

4.1.3. Excitation test results

Fig. 4.3 (a) and 4.3 (b) indicate the acceleration of the shaking table and the model (at the center of gravity), respectively, in the X direction when the input wave was Port Island. The green solid line was given when the model was not isolated, while the blue solid line was given when it was isolated. We have found that without seismic isolation, the acceleration of the unloader at its center of gravity is nearly twice that of the shaking table, but seismic isolation makes the former lower than the latter, indicating that the isolator has good isolation performance. Fig. 4.4 shows axial force acting on each of the unloader legs during the test. The green and blue solid lines represent the force without and with seismic isolation, respectively. LV1 to LV4 correspond to the same symbols shown in the right portion of Fig. 4.2. The red dashed line represents an axial force limit at which the leg does not float—if the axial force exceeds the limit, the leg floats. The red circles in Fig. 4.4 (a) and 4.4(d) show that the legs labeled LV3 and LV2 floated when they were without seismic isolation. On the contrary, we found that no leg floated with seismic isolation. Fig. 4.5 includes bar graphs that show the maximum acceleration, displacement, and axial force. In Fig. 4.5 (c), the axial force graph, 0 kN is defined as the load under which a leg starts to float; a positive value presses the leg to the ground, and a negative value lifts it. For all inputs, the displacement of the isolator did not exceed the allowable limit, and the isolator was effective in the reduction of acceleration acting on the unloader and in preventing the legs from floating.

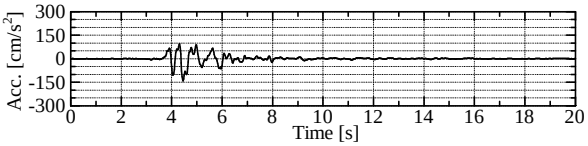

(a) Shaking table acceleration

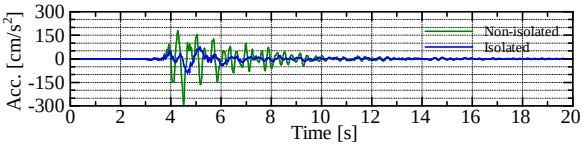

(b) Response accelerations of unloader when isolated and non-isolated

Figure 4.3. Experimental results for 50% Port Island input

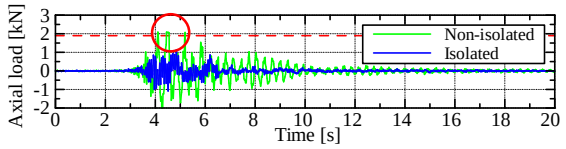

(a) LV3

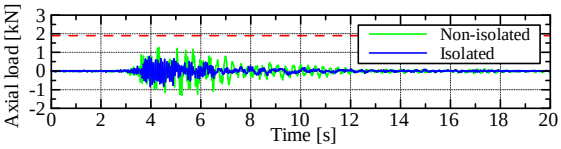

(b) LV4

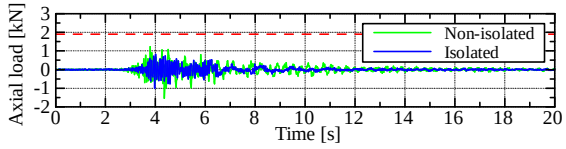

(c) LV1

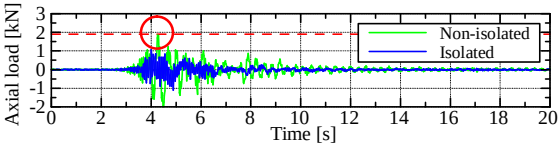

(d) LV2

Figure 4.4. Experimental result for axial loads of the unloader legs when isolated and non-isolated for 50% Port Island input

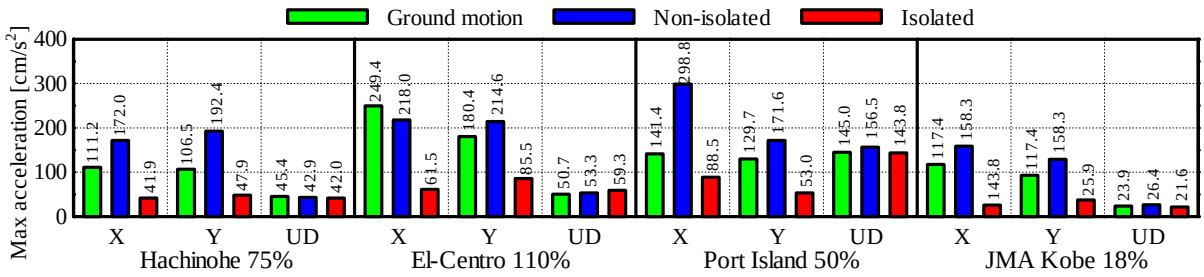

(a) Max accelerations

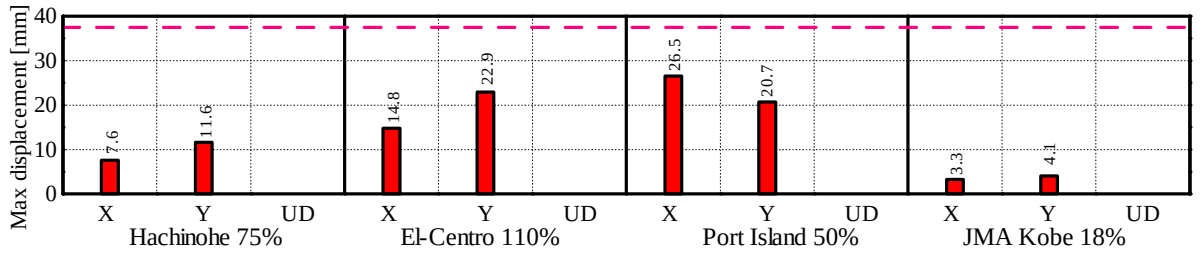

(b) Max displacements

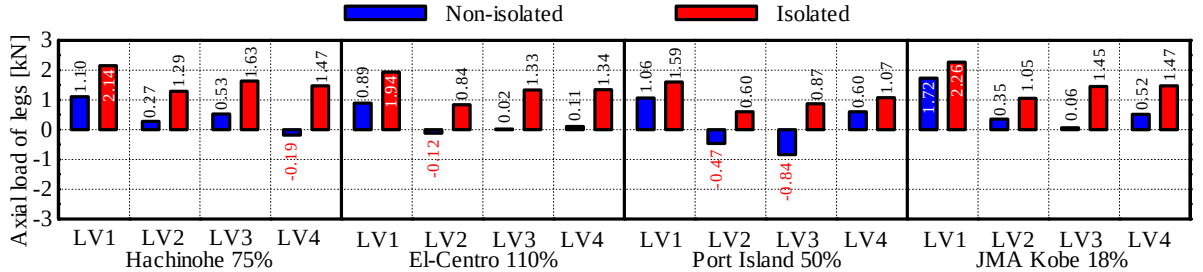

(c) Max axial loads of legs

Figure 4.5. Performance of isolation system for various inputs of shaking table

4.2. Simulation with FEM analysis

4.2.1. Analytical model

The unloader was a flexible structure, so we required an analytical model that took the 1st modes of the unloader without isolation into consideration. Therefore, we used FEM and analyzed the unloader without isolation to find the 1st modes in the X and Y directions and to develop a two-mass-system analytical model including the isolator. The two-mass system, a combination of the unloader and isolator, is represented by the following Eqn. 4.1:

$$\begin{bmatrix} m_0 & 0 \\ \beta_1 & 1 \end{bmatrix} \begin{Bmatrix} \ddot{x}_{dr0} \\ \ddot{\xi}_1 \end{Bmatrix} + \begin{bmatrix} c_0 & -c_c\phi_{c1} \\ 0 & 2\varsigma_1\omega_1 \end{bmatrix} \begin{Bmatrix} \dot{x}_{dr0} \\ \dot{\xi}_1 \end{Bmatrix} + \begin{bmatrix} k_0 & -k_c\phi_{c1} \\ 0 & \omega_1^2 \end{bmatrix} \begin{Bmatrix} x_{dr0} \\ \xi_1 \end{Bmatrix} = \begin{bmatrix} -m_0 \\ -\beta_1 \end{bmatrix} \ddot{x}_d \tag{4.1}$$

Table 4.4 lists the variables.

Table 4.4. Variable list

Var.	Description	Size	Var.	Description	Size
m_0	Mass of isolator's movable part	Scalar	c_0	Damping coefficient of isolator	Scalar
k_0	Spring constant of isolator	Scalar	x_{dr0}	Relative displacement of isolator with respect to ground	Scalar
x_d	Absolute displacement of ground	Scalar	c_c	Damping coefficient of connecting part between isolator and unloader	1×n matrix
k_c	Spring constant of connecting part between isolator and unloader	1×n matrix	ϕ_{c1}	1st modal vector of connecting part between isolator and unloader	n×1 matrix
β_1	1st mode participation factor of unloader	Scalar	ζ_1	1st modal damping factor of unloader	Scalar
ω_1	1st mode natural frequency of unloader	Scalar	ξ_1	1st modal displacement of unloader	Scalar

In this table, m_0, c_0, and k_0 are design values for the isolator, k_c, ϕ_{c1}, β_1, and ω_1 are derived from the results of the FEM modal analysis of the scale model, and c_c and ζ_1 are estimated from experience.

4.2.2. Comparing the excitation test and simulation results

We conducted a simulation with the parameters derived from the analytical model. Fig. 4.6 shows the comparison of the transfer functions of the X-direction acceleration from the shaking table to the center of gravity of the unloader. The green and blue solid lines represent the test and simulation results, respectively. The two results agree with each other well, which indicates that the proposed two-mass system simulation represents the characteristics of the real unit appropriately. This holds true for the Y direction, which is not shown in this paper. Fig. 4.7 to Fig. 4.9 indicate the test and simulation results for the responses including the acceleration, displacement, and axial force acting on each leg, when 75% Port Island input was used. In every graph, the green and blue solid lines represent the test and simulation results, respectively. In the displacement graph of the isolator, the orange chain lines represent the displacement limits. The two results are well consistent with each other in Fig. 4.7, which shows the acceleration of the unloader, Fig. 4.8, which presents the displacement of the isolator, and Fig. 4.9, which indicates the axial force on the unloader leg. This holds true for the other inputs. Accordingly, we have demonstrated that the proposed two-mass-system analytical model and analysis method yield a sufficiently precise simulation.

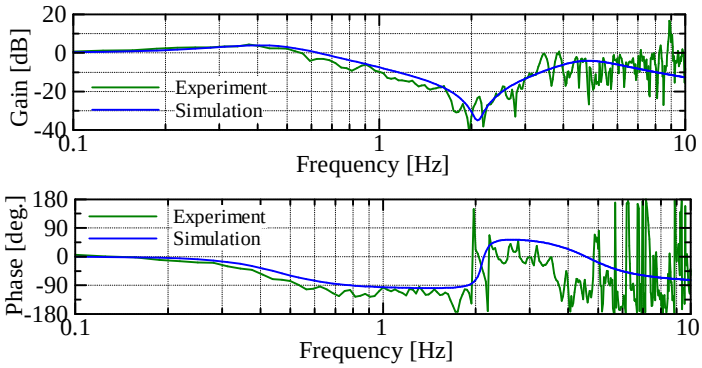

Figure 4.6. Transfer function from shaking table acceleration to response acceleration of unloader model (X direction)

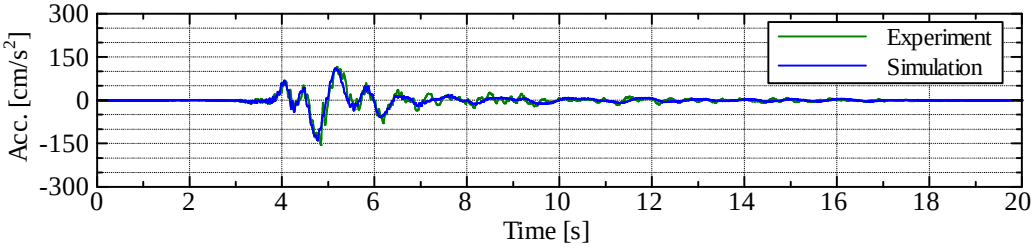

Figure 4.7. Experimental and analytical results of response acceleration for 75% Port-Island input (X direction)

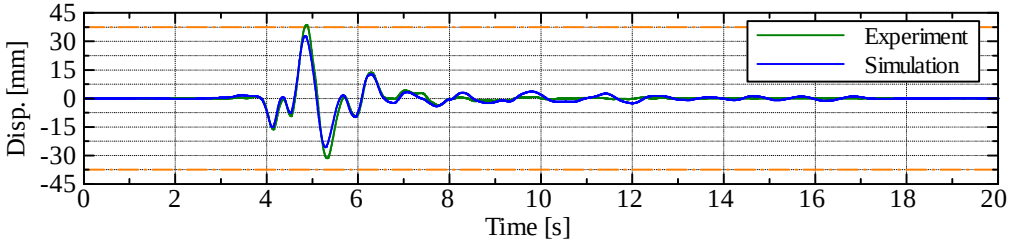

Figure 4.8. Experimental result and analytical results of isolator displacement for 75% Port-Island input (X direction)

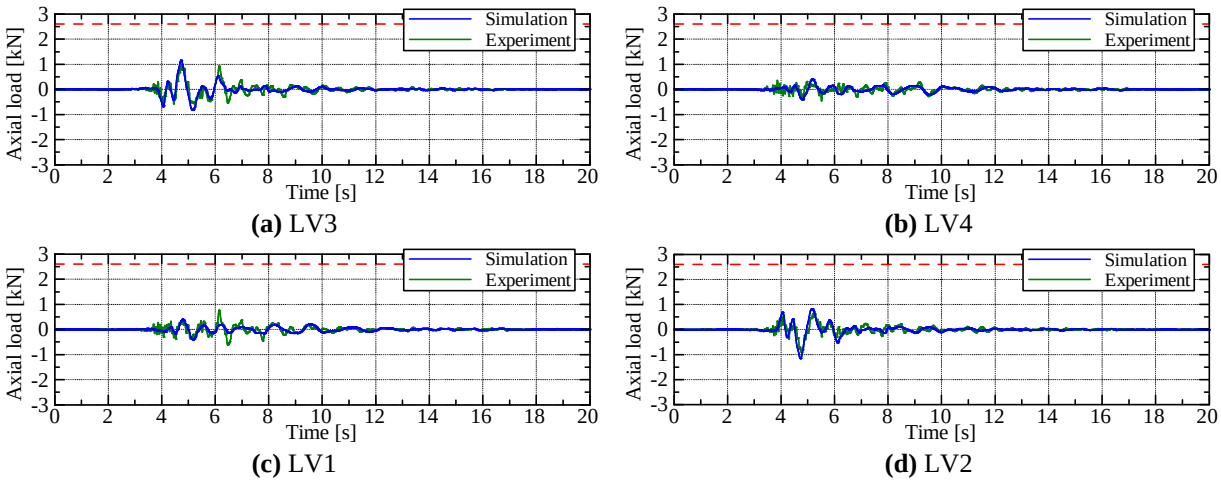

Figure 4.9. Experimental and analytical results of axial loads of the unloader legs for 75% Port-Island input (X direction)

5. CONCLUSIONS

In this study, we have developed a new two-dimensional seismic isolation system for unloaders, conducted a static force-application test of the full-scale model of the isolator and an excitation test of the scale model of an isolated unloader, and conducted a simulation analysis. The resultant conclusions are shown below.

(1) We have proposed a horizontal two-dimensional isolator for unloaders in which linear guides crossing each other at right angles support a vertical load, laminated rubber exerts restoration force, oil dampers having special structure produce damping force, and a locking mechanism functions.
(2) We have selected a typical unloader, designed and fabricated a full-scale isolator model, and conducted a static force-application test to check the isolator for correct functioning and reliability in strength.
(3) We have designed and fabricated a 1/8 scale model of the unloader including the isolator and conducted a shaking table test to confirm that the isolator has good seismic isolation performance.
(4) We have created a single-mass system that represents the 1st mode vibration characteristics derived from the FEM analysis and a two-mass-system model where the isolator is additionally taken into consideration, and conducted a simulation analysis to confirm that the model can analyze, with sufficient precision, the seismic response of the isolated unloader.

The results above have allowed us to design appropriate isolators for various unloaders by carrying out seismic response analysis with a two-mass-system model derived from the FEM analysis of the unloader.

ACKNOWLEDGEMENT

In the force-application test of the full-scale model and the excitation test of the scale model, Penta-Ocean Construction Co., Ltd. provided us with the static force-application tester and three-dimensional submerged shaking table. We express our sincere thanks the persons concerned.

REFERENCES

T. Fujimoto (1995). Mechanism of Damage to Port Facilities during 1995 Hyogo-ken Nanbu Earthquake (Part 2) Damages – Cargo Handling Facilities -. *Technical Note of the Port and Harbour Research Institute Ministry of Transport, Japan* **No. 813: Sept. 1995**, 77-93. (In Japanese)

H. Masuda., M. Abe, T. Koga, M. Hayatsu, M. Wada and T. Fujita. (2010). Effects of an Antiseismic Device and the Posture on Dynamic Seismic Behavior of Continuous Unloaders of Hinged Leg Structure. *Journal of Mechanical Systems for Transportation and Logistics* **Vol. 3: No. 3**, 477-492.

S. Iai (1989). Similitude for Shaking Table Tests on Soil-Structure-Fluid Model in 1g Gravitational Field. *Journal of the Japanese Society of Soil Mechanics and Foundation Engineering* **Vol. 29: No. 1**, 105-118.